On the effects of hydrocarbon and sulphur-containing compounds on the CCN activation of combustion particles

A. Petzold, M. Gysel, X. Vancassel, R. Hitzenberger, H. Puxbaum, S. Vrochticky, E. Weingartner, Urs Baltensperger, P. Mirabel

Atmos. Chem. Phys. Discuss., 5, 2599–2642, 2005
www.atmos-chem-phys.org/acpd/5/2599/
SRef-ID: 1680-7375/acpd/2005-5-2599
European Geosciences Union

Atmospheric Chemistry and Physics Discussions

On the effects of hydrocarbon and sulphur-containing compounds on the CCN activation of combustion particles

A. Petzold[1], M. Gysel[2], X. Vancassel[3], R. Hitzenberger[4], H. Puxbaum[5], S. Vrochticky[5], E. Weingartner[6], U. Baltensperger[6], and P. Mirabel[7]

[1]Institut für Physik der Atmosphäre, DLR Oberpfaffenhofen, 82234 Wessling, Germany
[2]School of Earth, Atmospheric and Environmental Sciences, University of Manchester, P.O. Box 88, Manchester M60 1QD, UK
[3]Atmospheric, Oceanic and Planetary Physics, University of Oxford, Clarendon Laboratory, Parks Road, Oxford OX1 3PU, UK
[4]Institute for Experimental Physics, Univ. of Vienna, Boltzmanngasse 5, 1090 Vienna, Austria
[5]Institute for Chemical Technologies and Analytics, Vienna University of Technology, Getreidemarkt 9/164UPA, Vienna, Austria
[6]Laboratory of Atmospheric Chemistry, Paul Scherrer Institut (PSI), 5232 Villigen, Switzerland
[7]Universite Louis Pasteur, 28, rue Goethe, 67000 Strasbourg, France

Received: 1 March 2005 – Accepted: 6 March 2005 – Published: 3 May 2005

Correspondence to: A. Petzold (andreas.petzold@dlr.de)

Abstract

The European PartEmis project ("Measurement and prediction of emissions of aerosols and gaseous precursors from gas turbine engines") was focussed on the characterisation and quantification of exhaust emissions from a gas turbine engine. A comprehensive suite of aerosol, gas and chemi-ion measurements were conducted under different combustor operating conditions and fuel sulphur concentrations. Combustion aerosol characterisation included on-line measurements of mass and number concentration, size distribution, mixing state, thermal stability of internally mixed particles, hygroscopicity, cloud condensation nuclei (CCN) activation potential, and off-line analysis of chemical composition. Modelling of CCN activation of combustion particles was conducted using microphysical and chemical properties obtained from the measurements as input data. Based on this unique data set, the role of sulphuric acid coatings on the combustion particles, formed in the cooling exhaust plume through either direct condensation of gaseous sulphuric acid or coagulation with volatile condensation particles nucleating from gaseous sulphuric acid, and the role of the organic fraction for the CCN activation of combustion particles was investigated. It was found that particles containing a large fraction of non-volatile organic compounds grow significantly less at high relative humidity than particles with a lower content of non-volatile OC. Also the effect of the non-volatile OC fraction on the potential CCN activation is significant. While a coating of water-soluble sulphuric acid increases the potential CCN activation, or lowers the activation diameter, respectively, the non-volatile organic compounds, mainly found at lower combustion temperatures, can partially compensate this sulphuric acid-related enhancement of CCN activation of carbonaceous combustion aerosol particles.

1. Introduction

The role of organic aerosols in the cloud formation is currently a very active scientific area. The effects of surface active and partially soluble organic compounds on the activation of aerosols to CCN are widely discussed (Saxena et al., 1995; Novakov and Corrigan, 1996; Facchini et al., 1999; Charlson et al., 2001; Broekhuizen et al., 2004), showing that these compounds tend to increase the CCN activation potential of a particle. The hydration properties of combustion particles were investigated mainly in terms of adsorption/desorption of water molecules (Chughtai et al., 1999; Popovitcheva et al., 2001; Seisel et al., 2004). These studies demonstrate that particles generated from sulphur containing fuels show higher hydration levels than combustion particles generated from sulphur free fuel (Chughtai et al., 1999). CCN activation studies on combustion particles including detailed chemical analysis of organic and inorganic compounds are scarce. Weingartner et al. (1997) investigated the hygroscopic growth behaviour of carbon and diesel soot particles, but without investigating the CCN activation. Lammel and Novakov (1995) investigated the water nucleation properties of carbon and diesel soot particles. They demonstrated that an increasing water-soluble fraction of the particles coincided with an enhanced CCN activation. However, an experimental study on the CCN activation potential of particles emitted from a combustion engine under real conditions, including particle processing in the exhaust gas is still missing.

During the European PartEmis project, a comprehensive suite of aerosol, gas and chemi-ion measurements were conducted under different combustion conditions and fuel sulphur concentrations (Wilson et al., 2004). Data sets on aerosol mass and number concentration, size distribution, mixing state, thermal stability of internally mixed particles, hygroscopicity, cloud condensation nuclei CCN activation potential and aerosol chemical composition were collected simultaneously from the exhaust of a gas turbine combustor (Petzold et al., 2003). Particular emphasis was put on the investigation of the connection between particle chemistry and the formation of cloud droplets on these combustion particles, because this CCN activation is the key process with

respect to any indirect effects of combustion-related particles on the global climate. Although the PartEmis project was dedicated to the investigation of particle formation and processing in aircraft engines, more general conclusions are investigated in this study with respect to the CCN activation of combustion particles emitted from a real-world combustion engine. This category of experiments is needed for providing the knowledge on particle formation and particle processing in the exhaust of a real combustion engine which cannot be gained from studies using laboratory flame burners. The study is thus expected to narrow the important gap of knowledge substantially, concerning particle emissions from an exemplary combustion source like an aircraft engine and their interaction with the atmosphere.

Two major scientific questions were addressed: 1/ Which role play volatile condensation particles forming in the cooling exhaust gas from sulphuric acid for the CCN activation potential of combustion particles? 2/ Which role plays the organic fraction of the combustion particles in the CCN activation potential? Targeted scientific objectives were thus aerosol microphysics and aerosol dynamics of combustion particles, formation of nucleation mode particles from the gas phase, interaction of combustion particles with gaseous and particulate sulphuric acid, speciation of the organic fraction of combustion particles, hygroscopic particle growth factors at water-subsaturated conditions, and CCN activation at well-defined water-supersaturated conditions. Modelling of CCN activation of combustion particles was conducted using microphysical and chemical properties obtained from the measurements as input data. Based on this unique data set, the importance of the chemical composition of the organic particle fraction and of the mass transfer of sulphuric acid from the gas phase to the combustion aerosol via condensation deposition and coagulation of nucleated particles and combustion particles was investigated with respect to the resulting CCN activation potential of the emitted carbonaceous combustion aerosol particles.

2. Experimental methods

2.1. Gas turbine combustor and exhaust sampling

In the framework of PartEmis, a gas turbine combustor was operated at two different operation conditions using fuel with three different fuel sulphur contents (50, 410, and 1270 mg kg^{-1}). The combustor operation conditions chosen correspond to modern and older engine gas path temperatures at cruise altitude of 35 000 feet (~11 700 m), and the medium fuel sulphur content is representative of the contemporary average of aviation fuel. The combustor behaved like a typical aircraft engine combustor with respect to thermodynamic data and main emissions. Table 1 summarises the operation conditions of the combustor.

A specially designed equal area traverse-sampling probe was used to extract exhaust samples from the combustor exit exhaust. The probe provided a radially averaged sample at each circumferential position of the combustor exit nozzle (see Fig. 1a for the shape of the exit nozzle). The sampling probe was moved stepwise, laterally across the combustor exit (eleven positions), where positions 1 and 11 were close to the combustor walls and position 6 was central. This approach allowed the lateral distribution of gaseous and aerosol species to be measured. A given operation condition and fuel sulphur content will hereinafter be referred to as a Combustor test condition, whereas each lateral sampling position will be referred to as a test point. In an aircraft engine gas turbine combustor, dilution air is fed into the combustion chamber downstream the combustion zone through holes in the chamber wall. As shown in Fig. 1b, the air to fuel ratio was distinctly higher and the combustor exit temperature T_{exit} was significantly lower at the outer sampling positions close to the chamber walls. This feature made additional investigations of the influence of the combustion temperature on particle composition and CCN activation potential possible. Mean emission properties were calculated for each Combustor test condition by weighting test point data with the respective air density at the exhaust gas temperature, see Fig. 1 and Wilson et al. (2004) for more details. The sampling probe was kept at each position for at least

20 min to allow for a sufficient sampling volume for each measurement method.

The sample was cooled to ~150°C within the water cooled sampling probe and delivered to undiluted and diluted sample lines. The undiluted line was insulated along its entire length in order to keep the temperature at ~150°C to avoid wall losses of combustion products, while the sample in the diluted line naturally attained room temperature (~25°C) after dilution. Filtered air at room temperature was used for sample dilution, and the dilution factor was determined from temperature and pressure corrected CO_2 concentrations measured in the supplied dilution air, diluted sample, and undiluted sample (Petzold et al., 2003; Wilson et al., 2004). The dilution factors during a Combustor test sampling probe traverse varied from 51 to 73 with a standard deviation of less than 10%. Although stable gaseous species such as CO_2 and water vapour are unaffected by intrusive sampling, aerosols may be lost due to diffusion and sedimentation to the surfaces of the sampling system. All on-line physical aerosol measurement methods and off-line aerosol chemical analysis methods deployed during the PartEmis experiments are summarised in Table 2 and detailed below.

2.2. On-line microphysical characterisation

On-line aerosol instruments were sampling from the diluted sample line, since dilution with filtered air was necessary for the majority of instruments to reduce concentrations below the upper detection limits. Microphysical properties, hygroscopic growth factors and CCN activation of the emitted combustion aerosol were simultaneously measured using in-situ methods. Thus artefacts from wall effects or sample storage could be excluded. In the case of filter samples, several test points were merged in order to meet the minimum required sample mass.

The basic aerosol properties used for this study were the number density and particle size distribution of the combustion aerosol (Petzold et al., 2003; Nyeki et al., 2004), the hygroscopic growth factors for defined particle dry sizes and relative humidity (Gysel et al., 2003), and the number of combustion particles activated as CCN at a saturation ratio with respect to water of 1.006–1.007 (Hitzenberger et al., 2003). The fraction of

CCN activated particles, or the activation ratio, respectively, was determined from the ratio of the number density of CCN and the number density N_{20} of combustion aerosol particles of size D>20 nm in the sampled gas. The lower cut-off diameter of 20 nm was chosen in order to focus exclusively on carbonaceous combustion aerosol particles and to exclude potentially nucleated condensation particles with typical diameters D<10 nm from the analysis (Petzold et al., 2003). The term CCN activation potential is used in the following for the fraction of CCN activated particles, because this ratio refers to a defined saturation ratio of 1.006–1.007, which is of the same order as saturation ratios met in natural liquid water clouds. However, when applied to real cloud conditions, the CCN activation ratio needs to be adapted to the saturation ratio prevailing in this particular cloud being investigated.

2.3. Off-line chemical analysis

Filter stack samplers and low pressure Berner impactors BLPI for total and size-segregated particulate matter chemical analysis were connected to the undiluted sampling line in order to obtain sufficient sampling volumes. The composition of the carbonaceous particle fraction was determined using both multi-step combustion methods for the determination of total carbon (TC) and elemental carbon (EC), and Evolved Gas Analysis methods EGA (Puxbaum, 1979) for measuring thermograms of the thermal stability of carbonaceous compounds. TC was measured with the multi-step combustion method by burning the entire filter sample and measuring the evolving CO_2. EC was determined according to Cachier et al. (1989) by oxidising the organic carbon (OC) during two hours of filter treatment at 340°C, the remaining carbonaceous material is then defined as EC. With the EGA, the CO_2 evolving at a given sample analysis temperature corresponds to the fraction of carbonaceous material which is oxidised at this temperature. Scanning the temperature up to approximately 850°C oxidises the complete carbonaceous material collected on the filter. A laser beam monitors the current transmittance of the filter sample. At the start of the EGA filters loaded with combustion particles are “black”, whereas they are expected to be “white” at the end of the EGA

when all collected carbonaceous material is oxidised. The combined thermo-optical method allows the distinction between OC and EC since the oxidisation of organic compounds up to approximately 500°C has no or little effect on the filter transmittance, while the oxidation of elemental carbon removes light-absorbing material and increases the filter transmittance.

The definitions for different classes of carbonaceous material are: i) semivolatile OC which evolves for T<300°C, ii) nonvolatile OC which evolves for T>300°C but does generally not influence the filter transmittance, and iii) EC which evolves at T>500°C and increases filter transmittance. The total carbon is TC=semivol OC+nonvol OC+EC. Black carbon (BC) was determined using Multi-Angle Absorption Photometry (Petzold and Schönlinner, 2004). To determine in particular SO_4^{2-}, two Dionex isocratic systems with electrochemical suppression were used.

3. Results and discussion

3.1. Composition of the carbonaceous fraction

Since the partitioning of carbonaceous compounds between the organic and elemental fractions is essential for this study, the reliability of the determined partitioning values was investigated by the two different approaches of evolved gas analysis and multi-step combustion. As is shown in Fig. 2, the ratio of EC to TC as determined by EGA methods is by approximately 15% lower than the ratio determined by multi-step combustion methods. However, this slight systematic difference between these two methods is well-known in the literature (Schmid et al., 2001). Furthermore, good agreement between EC from thermal methods and BC from aerosol absorption photometry was achieved with an average ratio of 1.05±0.06. The good agreement between EC / TC determined by two independent methods and between EC and BC, supports the high quality of carbon analysis methods conducted during PartEmis. All further discussions will refer to the carbonaceous compound classes defined above and determined by

EGA methods.

The OC fraction of TC depends on the exhaust gas temperature and thus on the air to fuel ratio and on the combustion temperature, see Fig. 3. Higher combustion temperature and thus a more complete combustion result in a lower OC fraction of TC. Exemplary thermograms are compiled in Fig. 4 for old and modern cruise conditions and different sectors of the combustor exit plane. While the EC peak dominates the spectrum for all cases, the intensity of semi- and nonvolatile OC peaks varies distinctly with the sampling probe position. Details of the partitioning of carbonaceous compound classes are summarised in Table 3 together with data on the combustor exit temperature, aerosol size distribution, and CCN activation. Figure 5 presents exemplary particle size distributions measured at edge and core positions of the exit plane. In contrast to the composition of the carbonaceous fraction, the variation in particle size distribution is less pronounced. However, a weak trend is visible from smaller particles at the edge positions or lower combustor exit temperatures, to larger particles at the centre position at a high combustor exit temperature. The OC/EC partitioning varies in parallel with the exhaust temperature laterally across the combustor exit nozzle test points. Any observed variation of the CCN activation across the combustor exit is hence expected to be mainly caused by variations of the OC/EC partitioning since the particle size distribution depends only weakly on the test point position.

Combining measured total carbon mass concentrations and respective aerosol volume and aerosol surface concentrations as calculated from the measured size distributions permits estimates of the particle density and particle specific surface area. The results are shown in Fig. 6 for the Combustor test data. The obtained median values for the particle density of 0.95 g cm^{-3} and for the particle surface area of 80 m^2 g^{-1} are close to values known for particles from other combustion sources. It has to be noted that the particles are not of spherical but of irregular shape. Hence, particularly the specific surface area reported here represents a lower estimate.

ACPD
5, 2599–2642, 2005

3.2. Sulphur-containing aerosol compounds

During combustion, the sulphur contained in the fuel is oxidised to SO_2 which is then partially converted to S(VI) in the hot exhaust gas. The efficiency of conversion from S(IV) to S(VI) is described by the conversion efficiency ε which was 2.3±1.2% during the PartEmis Combustor experiments (Katragkou et al., 2004). An unknown fraction of the gaseous sulphuric acid may become chemisorbed on the surface of the preexisting combustion aerosol particles, or it may condense on these particles during cooling of the exhaust gas. Size-segregated EC/TC partitioning and sulphate content of the combustion particles observed during PartEmis is shown in Fig. 7. The data originate from Berner low pressure impactor samples which were taken at a sample line temperature of 150°C. At these conditions most of the sulphuric acid will remain in the gas phase, while only a small fraction which is more strongly bound to the particle surface will be observed in particulate matter samples. The mass distribution of the carbonaceous matter matches the volume distribution of the aerosol, while the mass distribution of sulphate follows the surface distribution of the aerosol. Hence, the particulate sulphate at T~150°C is expected to be chemisorbed at the particle surface. The chemisorbed amount of sulphuric acid corresponds to a surface coverage of max. 0.1 monolayers in the high FSC case. In the low and medium FSC case, the coverage is far below 0.1 monolayer and thus below detection. The chemisorbed fraction of converted S(VI) corresponds to less than 0.1% of total S(IV) originally present in the fuel. With ε>1% more than 90% of the S(VI) remains in the gas phase at an exhaust temperature of about 150°C. The gaseaous S(VI) may then undergo reversible condensation deposition on preexisting particles or nucleation of new particles in the exhaust gas.

The coating of carbonaceous combustion particles by reversible condensation of H_2SO_4 was determined using Volatility Tandem DMA and Hygroscopicity Tandem DMA methods. Using the V-TDMA, the coating of particles by volatile matter is calculated from a shrinkage factor which describes the reduction in particle size when the volatile matter is vaporised (Nyeki et al., 2004). The H-TDMA method determines the vol-

ume fraction of soluble (sulphuric acid) matter from measurements of the hygroscopic growth behaviour as a function of relative humidity (Gysel et al., 2003). The coating thickness of combustion particles in terms of monolayers of sulphuric acid is plotted in Fig. 8. Both approaches give similar results which show, that only during the runs with high sulphur fuel the coating exceeded a single monolayer significantly. For particles in the CCN-relevant size range of 100 nm, the coating is almost negligible at low FSC and approaches a single monolayer at medium FSC. In the high FSC experiments, the total coverage of particles is about two monolayers of H_2SO_4 with only about 0.1 being chemisorbed.

Besides the carbonaceous combustion particles, also particles nucleated from gaseous precursors H_2SO_4 and H_2O were detected. These particles occurred preferably in the size range D<10 nm (Petzold et al., 2003). The formation of volatile particles by nucleation was strongly depending on the fuel sulphur content. No particle nucleation was observed in the low and medium fuel sulphur experiments, while strong nucleation was measured during the high sulphur fuel experiments. The right panel of Fig. 9 indicates that predominantly particles in the smallest diameter bin were affected by the fuel sulphur content. Modelling studies using these experimental observations (Vancassel et al., 2004) supported the hypothesis, that the particle nucleation took place downstream the Combustor exit when the sample air was diluted. Additional to the fuel sulphur content, another threshold condition for particle nucleation was the surface area of combustion particles being present in the exhaust gas. The carbonaceous aerosol surface area may act as an additional sink for condensable gases and suppress thus particle nucleation. Figure 9 indeed shows, that particle nucleation was only observed if the surface area was below a threshold of 2300 μm^2 cm^{-3}.

3.3. CCN activation of sulphuric acid-coated carbonaceous combustion particles

The chemical properties of the carbonaceous and the sulphur-containing particle fractions including nucleation mode particles were extensively described in the previous subsection. The effects resulting from variations of the organic fraction and the sulphur

coating of the carbonaceous combustion particles as well as the potential impact of nucleated H_2SO_4-H_2O particles on to the CCN formation potential of the combustion aerosol are discussed in this subsection.

The activation behaviour of combustion particles is described in terms of Köhler theory (Pruppacher and Klett, 1997). The Köhler equation relates the equilibrium gas phase saturation ratio S_w with respect to liquid water for a given solution droplet to its chemical composition or water activity a_w, respectively, and to the droplet size

$$S_w = a_w \times \exp\left[\frac{4\,M_w\sigma_{sol}}{RT\rho_w D_{eq}}\right]. \quad (1)$$

Water activity a_w and surface tension σ_{sol} of the solution are parameterised as a function of the particles chemical composition (Kulmala et al., 1997). M_w and ρ_w are water molecular weight and liquid water density. In the case of combustion aerosol covered by a sulphuric acid layer, the carbonaceous particle core is treated as an insoluble nucleus. The solution forming on the particle at a given saturation ratio S_w is composed of H_2SO_4 and H_2O. Depending on the water activity of the solution, the equilibrium water vapour pressure above the droplet may be below water saturation over a flat water surface (S_w<1), or above (S_w>1). The saturation ratio is often expressed as relative humidity RH=100×S_w in the subsaturated range. In the absence of soluble matter, the water activity term in the Köhler equation can be ignored, leaving the Kelvin equation describing the equilibrium S_w for a pure water droplet. The Kelvin equation also links the S_w to the critical size for droplet activation of an insoluble but wettable particle.

Basically two models have been deployed to calculate activation diameters for a combustion aerosol at a saturation ratio of 1.006 and resulting activation ratios for the measured size distributions. The roughest approximation is the assumption of an insoluble graphite core which undergoes a Kelvin-type activation process (Hitzenberger et al., 2003). A more sophisticated approach is based on a coated-sphere model, where the activation diameter is estimated from measured particle humidity growth factors (Gysel et al., 2003). This model uses experimental growth factor data and extrapolates

the observed growth behaviour up to the desired saturation ratios with respect to water. The only implicit assumption is that the particles consist of an insoluble core and a sulphuric acid coating.

The growth factor is defined as the ratio between the particle diameter at a certain saturation ratio and the particle diameter of the dry particle

$$g = \frac{D_{eq}(S_w)}{D_{dry}} = \frac{D_{eq}(RH)}{D_{dry}} \quad (2)$$

If the particle contains an insoluble core which is coated by a water-soluble layer of volume fraction ε_{sol}, only the water-soluble material can grow by water uptake (Gysel et al., 2003)

$$g(S_w, \varepsilon_{sol}) = \left[1 + \varepsilon_{sol}\left(g^3_{sol}(S_w) - 1\right)\right]^{\frac{1}{3}} \quad (3)$$

g_{sol} (S_w, ε_{sol}) denotes the theoretical growth factor for a pure soluble particle of equal wet size and can be calculated by Köhler theory.

The experimental particle growth factors were determined using the Hygroscopicity Tandem Differential Mobility Analyser technique H-TDMA (Weingartner et al., 2002; Gysel et al., 2002). Figure 10 shows growth curves for particles of dry size 100 nm, measured with a H-TDMA and modelled with Köhler theory. The volume fraction of water-soluble matter ε_{sol} was used as a fitting parameter. The obtained volume fractions were ε_{sol}<0.1% for low FSC, ε_{sol}=0.8–1.2% for medium FSC and ε_{sol}=2.7–3.0% for high FSC. Respective values for smaller particles are given by Gysel et al. (2003).

Substituting D_{eq} by $g \times D_{dry}$ in Eq. (1) yields the modified Köhler equation

$$S_w = a_w \times \exp\left[\frac{4 M_w \sigma_{sol}}{RT \rho_w g(S_w, \varepsilon_{sol}) D_{dry}}\right] \quad (4)$$

From this equation, the equilibrium water vapour pressure can be calculated over particles, consisting of an insoluble core and a layer of water-soluble sulphuric acid of volume fraction of ε_{sol}.

Figure 11 shows these so-called Köhler curves for various values of ε_{sol} and a given dry size D_{dry}=100 nm The grey shaded area indicates the saturation ratio with respect to water at which the CCN counter used during PartEmis (Giebl et al., 2002) was operated. The drop diameter corresponding to the maximum S_w value, or critical saturation ratio respectively, is the critical diameter which is required for droplet activation at S_w. The mid panel of Fig. 11 shows the corresponding critical saturation ratios required for the activation of a coated particle of size D_{dry} for droplet formation. The impact of the sulphuric acid coating of the combustion particles on their activation for cloud droplet formation becomes clearly visible.

For the experimental determination of the activation diameter, the number of droplets forming in the CCN counter was normalised to the number of combustion particles entering the counter. The corresponding number size distributions were integrated from the maximum diameter 0.5 μm to smaller sizes until the integrated fraction equalled the activation ratio N_{CCN}/N_{20}. The threshold diameter is the measured critical activation diameter D_{CCN}, i.e.,

$$\frac{N_{CCN}}{N_{20}} = \frac{\int_{D_{CCN}}^{0.5} n(D) d \log D}{\int_{0.02}^{0.5} n(D) d \log D} \quad (5)$$

Table 3 contains the CCN activation diameters obtained from Eq. (4). As is demonstrated in the bottom panel of Fig. 11, all average activation diameters determined for the different fuel sulphur runs of the combustor agree well with a saturation ratio of 1.006 inside the CCN counter. This saturation ratio is of similar magnitude as observed in natural liquid water clouds. The additional lines in Fig. 11 represent the activation diameters calculated for saturation ratios of 1.01 and 1.05. These high values are reached in the initial state of contrail formation (Kärcher et al., 1996).

Table 4 summarises the activation ratios expected for a typical combustion aerosol size distribution as measured in the exhaust of the PartEmis combustor. Values are compiled for pure insoluble graphite particles without coating (ε_{sol}=0%) and for combustion particles coated with 3 vol.-% sulphuric acid. Considered cases are a liquid

water cloud at S_w=1.006 and a contrail in its early stage at S_w=1.05. The values at S_w=1.01 are added for comparison with literature data (Lammel and Novakov, 1995). The coating of graphite particles with sulphuric acid increases the activation ratio for liquid water cloud conditions by more than two orders of magnitude from $\leq 10^{-4}$ to $>10^{-2}$. However, even coated but young combustion particles from gas turbines are still poor CCN.

At high saturation ratios of 1.05 occurring in very young contrails, about one fourth of all particles become activated if they are not coated. In the case of coated particles, every second particle becomes activated. Since for S_w=1.006 D_{CCN} is positioned at the large-size tail of the size distribution, a small decrease in D_{CCN} has a large effect on the activation ratio. In contrast, the activation diameter for contrail conditions of S_w=1.05 lies close to the maximum of the size distribution. Thus, a decrease in D_{CCN} has only a weak effect on the activation ratio. It is known from observations in contrails, that 1/3 of emitted combustion particles are incorporated into or attached to contrail ice particles (Petzold et al., 1997; Schröder et al., 1998; Kuhn et al., 1998). This fraction of combustion particles associated with the contrail ice phase at cruise altitude is in remarkably close agreement with the conclusions drawn from the PartEmis experiment for the activation of combustion particles in contrails. The activation ratio increases from 0.25 for pure insoluble particles to $\geq$0.5 for coated particles which is a factor of 2. Referring to the observations of the impact of the fuel sulphur content on the properties of contrails (Petzold et al., 1997), only a weak effect of the FSC on the number of contrail particles was found. The number of ice crystals in the contrail of the ATTAS aircraft increased from 1500 to 2000 particles per cm^3 when the fuel sulphur content was increased from 2 to 2700 mg kg^{-1}.

Lammel and Novakov (1995) reported activation ratios at a saturation ratio S_w=1.01 ranging from 1 to >80% for different types of combustion particles. The observation of 2% activated particles with 3 vol.-% of coating corresponds to the reported activation ratio of 1% from Aviation fuel JP-4. A similar value of 1% of CCN activated particles emitted from aircraft engines is reported by Pitchford et al. (1991) from in

situ measurements. Diesel particles and particles from wood smoke which contain higher fractions of water soluble matter exhibit a much higher CCN activation with activated fractions of 25–80%. CCN activation diameters reported by Lammel and Novakov (1995) for S_w=1.005 are 140 nm for diesel engine exhaust, which is very close to the values reported in this study, and 60–120 nm for treated and untreated carbon black particles. Similar to the presented results, the activation diameter decreased with increasing water-soluble fraction of the particle.

3.4. Effect of nucleation mode particles on the CCN activation

For the high fuel sulphur content experiments, the effect of particle nucleation on the CCN activation of the combustion aerosol was investigated. The underlying question was whether additional transfer of water soluble matter from the gas phase to the surface of the combustion particles by particle nucleation and subsequent coagulation with combustion particles will have a significant effect on the CCN activation potential of the combustion particles. In the course of the modelling studies on particle nucleation (Vancassel et al., 2004), the mass transfer of H_2SO_4 from the gas phase to the surface of the combustion particles was calculated for test points at high FSC conditions without and with particle nucleation events.

During test points without particle nucleation the only active H_2SO_4 deposition process is gas phase deposition by diffusion. These test points were used as reference cases. It turned out that 60–65% of the total number of H_2SO_4molecules were deposited on the combustion aerosol surface by deposition from the gas phase, while the remaining 35–40% were deposited by particle coagulation. For the high FSC cases, approximately 1.8 to 1.9 vol.-% of the water soluble matter are assumed to result from gas phase deposition while 1.1 to 1.2% are contributed by particle coagulation. This estimate corresponds to 65% of the ensemble value ε_{sol}=3.0 vol.-% determined by the Köhler curve fitting all measurements.

The left panel of Fig. 12 shows the experimentally determined CCN activation diameters for the high FSC runs as a function of the ratio of nucleated particles N_{NUC}

to combustion particles $N_{COMBUSTION}$ for the high fuel sulphur case. The right panel of Fig. 12 shows the volume fraction of soluble matter calculated from the measured D_{CCN} values using Köhler theory (Eq. 3). These values are in close agreement with the ensemble value ε_{sol}. Furthermore, the minimum gas-phase deposition coating of 1.8 to 1.9 vol.-% estimated from the model calculations agrees well with the coating estimated from the CCN activation diameter for the lowest ratio $N_{NUC}/N_{COMBUSTION}$.

Since the ratio $N_{NUC}/N_{COMBUSTION}$ is a measure for the strength of particle nucleation, a significant influence of particle nucleation and subsequent coagulation on the CCN activation potential of the combustion aerosol is observed. The activation diameter is lowered from 155 nm without coagulation mass transfer to 126 nm at maximum particle nucleation. Similarly, the particle coating increases from 2 vol.-% to maximum 4 vol.-%. The reduction in D_{CCN} by additional mass transfer of water soluble matter via particle coagulation is if the order of 20% at S_w=1.006.

3.5. CCN activation of combustion particles with a high OC fraction

The humidity growth factors and resulting CCN activation diameters for the different experimental parameters, i.e., old and modern conditions and fuel sulphur content levels, were determined from one set of data points at each experimental condition. Each data set consisted of humidity growth factors which were measured during the scan of the sampling probe across the nozzle exit plane. The overall humidity growth behaviour of the combustion particles at the given experimental condition was determined from the entire data set, as can be seen in Fig. 10.

The scans of the sampling probe included the edge positions, which showed a significant deviation in the OC-fraction of TC compared to the samples from the centre of the nozzle exit plane. Figure 13 demonstrates exemplary that not only the OC-TC fraction was different for particles sampled at the edge positions, but also the growth behaviour. This observation was a first indicator of a likely influence of the OC fraction of TC on the growth behaviour of combustion particles. In order to investigate whether there is an impact of the OC fraction of TC on the CCN activation, the activation di-

ameters measured at each sampling probe position were normalised to the ensemble value D_{CCN} (ensemble) represented by the Köhler curve fitting all measurements (see Fig. 11, bottom panel). In Fig. 14, these ratios D_{CCN}(exp)/D_{CCN} (ensemble) are plotted as function of the semivolatile OC fraction of TC (left) and the non-volatile OC fraction of TC (right).

An increasing fraction of non-volatile OC compounds increases D_{CCN} which in turn reduces the potential of combustion particles for CCN activation significantly. For the semivolatile OC no such trend is observable. The maximum increase in D_{CCN} with respect to D_{CCN}(ensemble) is ≅30% which translates into a reduction of the activation ratio from 2×10^{-3} to 9×10^{-4} for particles coated with 0.8 vol.-% sulphuric acid. Table 5 summarises the effects of particle coating and organic content on the CCN activation of combustion particles, based on the observations during PartEmis. Already a large effect occurs at the transition from the pure insoluble particle to the particle coated weakly with water-soluble substances.

As a final assessment of the competing effects of sulphur-containing and organic compounds on the CCN activation of combustion particles, the reduction of the activation diameter with respect to a Kelvin-type activation of insoluble graphite particles is plotted in Fig. 15. Coating the insoluble particle with 0.1 volume-% of sulphuric acid reduces the activation diameter by 15% with respect to Kelvin type activation. For approx. 1.0 and 3.0 vol.-% coating, respectively, the reduction of D_{CCN} is 50% and 60%. Coating thickness enhancement through coagulation with nucleation mode sulphuric acid-water particles further reduces the CCN activation diameter to 36% of the Kelvin-type reference D_{CCN}. In contrast, a high fraction of nonvolatile organic compounds increases the activation diameter by maximum 30% compared to a similar case with low non-volatile OC content. Summarising, a large fraction of nonvolatile organic compounds of combustion aerosol particles has a significant effect on the potential CCN activation. While a coating with water-soluble sulphuric acid increases the CCN activation potential, or reduces the activation diameter, respectively, the organic compounds can compensate this sulphuric acid-related enhancement of the CCN activation poten-

tial by about one third of the effect.

4. Summary and conclusions

In the course of the European experiment PartEmis the CCN activation of combustion particles generated in a gas turbine combustor was investigated. The presented analysis of the experimental and modelling data showed, that pure carbonaceous particles emitted from a gas turbine combustor are very poor CCN which behave very similar to insoluble particles undergoing a Kelvin-type activation process. For almost pure carbonaceous particles only a fraction of 10^{-4} becomes activated to CCN. Increasing the coating of the particles with water soluble H_2SO_4 to 3% of the particle volume increases the potential CCN activation at a saturation ratio of 1.006 by about two orders of magnitude. The presence of nucleated H_2SO_4-H_2O particles enhances the mass transfer of water soluble sulphuric acid from the gas phase to the surface of the combustion particles by particle coagulation, which results in a further reduction of the CCN activation diameter. On the other hand, a high fraction of non-volatile organic matter in the particles causes a considerable increase in the activation diameter. However, the reduction of the CCN activation potential of the combustion particles by the non-volatile OC fraction can balance the increase in the potential activation by coating with H_2SO_4 only to some extent. Although the data are obtained from particles emitted from a gas turbine combustor, the competing effects of OC reducing CCN activation and coating with water soluble matter increasing CCN activation are considered important also for combustion particles emitted from other sources.

The presented analysis is far from being quantitative, and the experimental data are limited. However, it presents important experimental material for the discussion on how organic components influence the CCN activity of internally mixed particles. Research on this subject focused so far on the role of organic acids and water soluble organic matter. The experiments showed that soluble organic compounds activate according to Köhler theory whereas highly insoluble species do not activate at atmo-

spherically relevant super-saturations (e.g., Novakov and Corrigan, 1996; Giebl et al., 2002; Broekhuizen et al., 2004). Comparing CCN activation diameters of organic acids at S_w=1.005 (Corrigan and Novakov, 1999) with the values reported here shows, that even less active organic acids like adipic acid exhibit D_{CCN} values of 116 nm, while even coated combustion particles activate only for sizes larger than $D_{CCN} \cong 140$ nm. For an urban aerosol which likely contains larger fractions of combustion particles, Saxena and co-workers (1995) reported that organic compounds diminish water adsorption of the inorganic fraction by about 30%, while for non-urban aerosol the organic fraction increases the water adsorption. The PartEmis results indicate an effect of the organic fraction on the CCN activation potential similar to urban aerosol which contains a considerable fraction of combustion particles. Furthermore, the CCN activation of pure and coated carbon black particles was recently investigated using particles which were produced by nebulising an aqueous suspension of carbon black in a collision atomizer (Dusek et al., 2005[1]). The activation of pure carbon black particles was found to require higher saturation ratios than predicted by Kelvin theory for insoluble, wettable spheres. Theoretical calculations indicated that the deviation of measured activation from Kelvin theory was consistent with a non-zero contact angle of the order of 4–6° of water at the soot surface. Coating the soot particles with a small amount of NaCl by adding 5% by mass NaCl to the carbon black suspension greatly enhanced their CCN efficiency. The measured CCN efficiencies were consistent with Köhler theory for particles consisting of insoluble and hygroscopic material. The PartEmis results for combustion particles point in the same direction as the observations for urban aerosol particles and carbonaceous particles generated in the laboratory.

The effect of particle ageing in the atmosphere which tends to increase the CCN activation potential due to oxidation of the particle surface was investigated by Hallett and co-workers (1989) for particles emitted from kerosene flames. 24 h of ageing increased the ratio CCN/N only from <2% to 3%. Similar investigations of the influence

[1]Dusek, U., Ctyroky, P., Reischl, G., and Hitzenberger, R.: CCN activation of pure and coated carbon black particles, in preparation, 2005.

of particle ageing on the CCN activation potential of combustion particles were not performed during PartEmis. Translating the ageing results from Hallet et al. to the PartEmis aerosol suggests that by far the major contribution to the CCN activation potential of combustion particles can be assigned to the coating with water-soluble matter which increases the ratio CCN/CN by two orders of magnitude at S_w=1.006.

Acknowledgements. The PartEmis project was funded by the European Commission and by the Swiss Bundesamt für Bildung und Wissenschaft under contracts no. G4RD-CT-2000-00207 and 99.0632, respectively. The authors are very grateful to C. W. Wilson and the test rig operation crew at QinetiQ for their very strong support during the experiments. Valuable contributions from C. Stein and L. Fritzsche (DLR), as well as from H. Giebl (University of Vienna) during the analysis of the PartEmis data set are gratefully acknowledged.

References

Broekhuizen, K., Pradeep Kumar, P., and Abbatt, J. P. D.: Partially soluble organics as cloud condensation nuclei: Role of trace soluble and surface active species, Geophys. Res. Lett., 31, L01107, doi:10.1029/2003GL018203, 2004.

Cachier, H., Bremond, M. P., and Biat-Ménard, P.: Determination of atmospheric soot carbon with a simple thermal method, Tellus, 41B, 379–390, 1989.

Charslon, R. J., Seinfeld, J. H., Nenes, A., Kulmala, M., Laaksonen, A., and Facchini, M. C.: Reshaping the theory of cloud formation, Science, 292, 2025–2026, 2001.

Chughtai, A. R., Miller, N. J., Smith, D. M., and Pitts, J. R.: Carbonaceous particle hydration III, J. Atmos. Chem., 34, 259–279, 1999.

Corrigan, C. E. and Novakov, T.: Cloud condensation nucleus activity of organic compounds: a laboratory study, Atmos. Environ., 33, 2661–2668, 1999.

Facchini, M. C., Mircea, M., Fuzzi, S., and Charlson, R. J.: Cloud albedo enhancement by surface-active organic solutes in growing droplets, Nature, 401, 257–259, 1999.

Giebl, H., Berner, A., Reischl, G., Puxbaum, H., and Hitzenberger, R.: CCN activation of oxalic acid and malonic acid test aerosols with the Univ. of Vienna cloud condensation nuclei counter, J. Aerosol Sci., 33, 1623–1634, 2002.

Gysel, M., Weingartner, E., and Baltensperger, U.: Hygroscopicity of Aerosol particles at low temperatures: 2. Theoretical and experimental hygroscopic properties of laboratory generated aerosols, Environ. Sci. Technol., 36, 63–68, 2002.

Gysel, M., Nyeki, S., Weingartner, E., Baltensperger, U., Giebl, H., Hitzenberger, R., Petzold, A., and Wilson, C. W.: Properties of jet engine combustor particles during the PartEmis experiment, Hygroscopicity at subsaturated conditions, Geophys. Res. Lett., 30, 1566, doi:10.1029/2003GL016896, 2003.

Hallet, J., Hudson, J. G., and Rogers, C. F.: Characterization of combustion aerosols for haze and cloud formation, Aerosol Sci. Technol., 10, 70–83, 1989.

Hitzenberger, R., Giebl, H., Petzold, A., Gysel, M., Nyeki, S., Weingartner, E., Baltensperger, U., and Wilson, C. W.: Properties of jet engine combustor particles during the PartEmis experiment, Hygroscopic properties at supersaturated conditions, Geophys. Res. Lett., 30, 1779, doi:10.1029/2003GL017294, 2003.

Katragkou, E., Wilhelm, S., Arnold, F., and Wilson, C. W.: First gaseous Sulfur (VI) measurements in the simulated internal flow of an aircraft gas turbine engine during project PartEmis, Geophys. Res. Lett., 31, 2117, doi:10.1029/2003GL018231, 2004.

Kärcher, B., Peter, Th., Biermann, U. M., and Schumann, U.: The initial composition of jet condensation trails, J. Atmos. Sci., 53, 3066–3083, 1996.

Kuhn, M., Petzold, A., Baumgardner, D., and Schröder, F. P.: Particle composition of a young condensation trail and of upper tropospheric background aerosol, Geophys. Res. Lett., 25, 2679–2682, 1998.

Kulmala, M., Vesala, T., and Kalkinnen, J.: Data for phase transitions in aerosol systems Manuscript for laboratory use, University of Helsinki, Helsinki, 1997.

Lammel, G. and Novako, T.: Water nucleation properties of carbon black and diesel soot particles, Atmos. Environ., 29, 813–823, 1995.

Novakov, T. and Corrigan, C. E.: Cloud condensation nucleus activity of the organic component of biomass smoke particles, Geophys. Res. Lett., 23, 2141–2144, 1996.

Nyeki, S., Gysel, M., Weingartner, E., Baltensperger, U., Hitzenberger, R., Petzold, A., and Wilson, C. W.: Properties of jet engine combustion particles during the PartEmis experiment: Particle size spectra (d>15 nm) and volatility, Geophys. Res. Lett., 31, L18105, doi:10.1029/2003GL020569, 1–4, 2004.

Petzold, A., Busen, R., Schröder, F. P., Baumann, R., Kuhn, M., Ström, J., Hagen, D. E., Whitefield, P. D., Baumgardner, D., Arnold, F., Borrmann, S., and Schumann, U.: Near field

measurements on contrail properties from fuels with different sulfur content, J. Geophys. Res., 102, 29 867–29 880, 1997.
Petzold, A., Ström, J., Ohlsson, S., and Schröder, F. P.: Elemental composition and morphology of ice crystal residual particles in cirrus clouds and contrails, Atmos. Res., 49, 21–34, 1998.
Petzold, A., Stein, C., Nyeki, S., Gysel, M., Weingartner, E., Baltensperger, U., Giebl, H., Hitzenberger, R., Döpelheuer, A., Vrchoticky, S., Puxbaum, H., Johnson, M., Hurley, C. D., Marsh, R., and Wilson, C. W.: Properties of jet engine combustor particles during the PartEmis experiment, Microphysical and chemical properties, Geophys. Res. Lett., 30, 1719, doi:10.1029/2003GL017283, 2003.
Petzold, A. and Schönlinner, M.: Multi-angle absorption photometry – a new method for the measurement of aerosol light absorption and atmospheric black carbon, J. Aerosol Sci., 35, 421–441, 2004.
Pitchford, M., Hudson, J. G., and Hallet, J.: Size and critical supersaturation for condensation of jet engine exhaust particles, J. Geophys. Res., 96, 20 787–20 793, 1991.
Popovitcheva, O. B., Trukhin, M. E., Persiantseva, N. M., and Shonija, N. K.: Water adsorption on aircraft-combustor soot under young plume conditions, Atmos. Environ., 35, 1673–1676, 2001.
Pruppacher, H. R. and Klett, J. D.: Microphysics of Clouds and Precipitation, Kluwer 2nd edition, Academic Publishers, Dordrecht, 1997.
Puxbaum, H.: Thermo-Gasanalysator zur Charakterisierung von Kohlenstoff und Schwefelverbindungen in luftgetragenen Stäuben, Fresenius Z. Anal. Chem., 298, 250–259, 1979.
Saxena, P., Hildemann, L. M., McMurry, P. H., and Seinfeld, J. H.: Organics alter hygroscopic behaviour of atmospheric particles, J. Geophys. Res., 100, 18 755–18 770, 1995.
Schmid, H., Laskus, L., Abraham, H. J., Baltensperger, U., Lavanchy, V., Bizjak, M., Burba, P., Cachier, H., Crow, D., Chow, J., et al.: Results of the "carbon conference" international aerosol carbon round robin test stage I., Atmos. Environ., 35, 2111–2121, 2001.
Schröder, F. P., Kärcher, B., Petzold, A., Baumann, R., Busen, R., Hoell, C., and Schumann, U.: Ultrafine aerosol particles in aircraft plumes: In situ observations, Geophys. Res. Lett., 25, 2789–2793, 1998.
Seisel, S., Lian, Y., Keil, T., Trukhin, M. E., and Zellner, R.: Kinetics of the interaction of water vapour with mineral dust and soot surfaces at T = 298 K, Phys. Chem. Chem. Phys., 6, 1926–1932, 2004.
Vancassel, X., Sorokin, A., Mirabel, P., Petzold, A., and Wilson, C. W.: Volatile particles forma-

tion during PartEmis: a modelling study, Atmos. Chem. Phys., 4, 439–447, 2004, SRef-ID: 1680-7324/acp/2004-4-439.
Weingartner, E., Burtscher, H., and Baltensperger, U.: Hygroscopic properties of carbon and diesel soot particles, Atmos. Environ., 31, 2311–2327, 1997.
Weingartner, E., Gysel, M., and Baltensperger, U.: Hygroscopicity of aerosol particles at low temperatures: 1. New low-temperature H-TDMA instrument: Setup and first applications, Environ. Sci. Technol., 36, 55–62, 2002.
Wilson, C. W., Petzold, A., Nyeki, S., Schumann, U., and Zellner, R.: Measurement and Prediction of Emissions of Aerosols and Gaseous Precursors from Gas Turbine Engines (PartEmis): An Overview, Aerospace Sci. Technol., 8, 131–143, 2004.

Table 1. Combustor operating conditions during the PartEmis Combustor experiments.

Combustor Parameters	Old	Modern
Tcombustor inlet, K	566	766
Tcombustor outlet, K	1125	1448
P combustor inlet, 10^5 Pa	7.05	8.2
Air mass flow, kg s^{-1}	2.12	2.12
Fuel flow, kg s^{-1}	0.032	0.042
Air fuel ratio	66	50.3

Table 2. Deployed equipment and measured aerosol properties.

Aerosol property	Technique
On-line methods	
Volatile condensation particles (number, size)	Condensation Particle Size Analyser (CPSA, Stein et al., 2001; Petzold et al., 2003), Differential Mobility Analyser (DMA) connected to a Thermodenuder
Non-volatile carbonaceous particles (number, size)	Condensation Particle Counter (CPC), Scanning Mobility Particle Sizer (SMPS), DMA connected to a Thermodenuder Volatility Tandem-DMA (Nyeki et al., 2004)
Aerosol absorption coefficient σ_{ap}	Multi-Angle Absorption Photometer (Petzold and Schönlinner, 2004)
Water uptake at RH≤100%	Hygroscopicity Tandem-DMA (Gysel et al., 2002)
Cloud condensation nuclei	Thermal gradient CCN counter (Giebl et al., 2002)
Off-line methods	
Chemical composition	Berner low pressure impactor (BLPI) samples; filter stack samples; sample analysis via – gravimetry (total mass), – multi-step combustion method (organic/elemental carbon), – evolved gas analysis (volatility of carbonaceous compounds) – gas chromatography (aliphatic constituents), – ion chromatography (major ions).

Table 3. Results for the medium FSC experiment (FSC=0.41 g kg^{-1}) concerning the partitioning of carbonaceous compounds between semivolatile OC, non-volatile OC and EC, particle size distribution (CMD=count median diameter, GSD=geometric standard deviation), CCN activation ratio CCN/N_{20}, and activation diameter D_{CCN} at S_w=1.006 as estimated from the measured size distribution and activation ratio.

Condition	Probe Position	T_{exit} K	semivol. OC/TC	nonvol. OC/TC	EC/TC	CMD nm	GSD	CCN/N_{20} $\times 10^{-3}$	D_{CCN} nm
OLD	11	852	0.17	0.44	0.39	33	1.67	0.67	240
	10	1172	0.18	0.38	0.44	38	1.62	1.24	193
	9–7	1236	0.25	0.32	0.43	40	1.72	1.40	192
	6	1267	0.14	0.32	0.54	51	1.59	1.52	219
	5–3	1308	0.11	0.40	0.49	40	1.65	1.46	199
	1	1007	0.32	0.31	0.37	36	1.64	1.11	196
MODERN	11	1189	0.20	0.52	0.28	36	1.69	2.28	182
	9–7	1652	0.10	0.40	0.50	42	1.66	3.71	174
	6	1623	0.08	0.34	0.58				
	5–3	1585	0.11	0.41	0.48	41	1.70	3.14	186
	1	1201	0.19	0.50	0.31	47	1.73	2.76	207

Table 4. Activation ratios N_{CCN}/N for liquid water clouds and Contrails for pure insoluble particles (ε_{sol}=0%) and coated combustion particles (ε_{sol}=3%).

	S_w	ε_{sol}	D_{CCN}, nm	N_{CCN}/N
Water cloud	1.006	0%	360	$\leq 10^{-4}$
		3%	142	$(7\pm1)\times10^{-3}$
	1.01	0%	215	3×10^{-4}
		3%	94	0.02
Contrail	1.05	0%	44	0.23
		3%	27	0.53

Table 5. Activation diameter D_{CCN} and activation ratio N_{CCN}/N for the investigated coated and non-coated combustion particles for a saturation ratio S_w=1.006.

Particle type	Coating ε_{sol}, %	Activation diameter D_{CCN}, nm	Activation ratio N_{CCN}/N
Insoluble	0	360	10^{-4}
H_2SO_4 – coated	0.1	290±43	$(8\pm2)\times10^{-4}$
H_2SO_4 – coated	0.8	190±12	$(2\pm0.6)\times10^{-3}$
H_2SO_4 – coated	1.2	178±14	$(4\pm1)\times10^{-3}$
H_2SO_4 – coated,	0.8	237	9×10^{-4}
nonvol. OC fraction = 0.5	1.2	205	3×10^{-3}
H_2SO_4 – coated	2.7	144±6	$(7\pm1)\times10^{-3}$
H_2SO_4 – coated	3.0	142±9	$(1\pm0.5)\times10^{-2}$

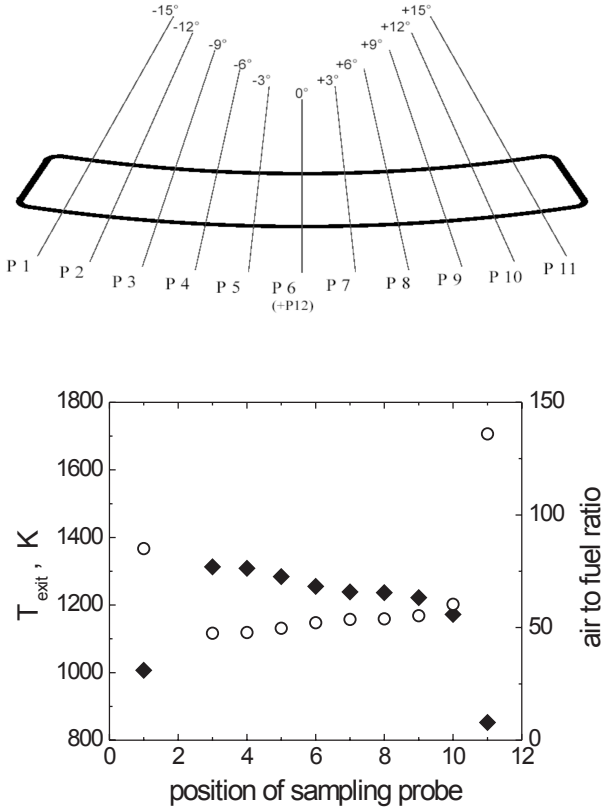

Fig. 1. Combustor exit temperature T_{ext} (filled symbols) and ratio of air to fuel (open symbols) for the sampling probe positions on the combustor exit nozzle plane (upper panel) during operation at old cruise conditions.

ACPD
5, 2599–2642, 2005

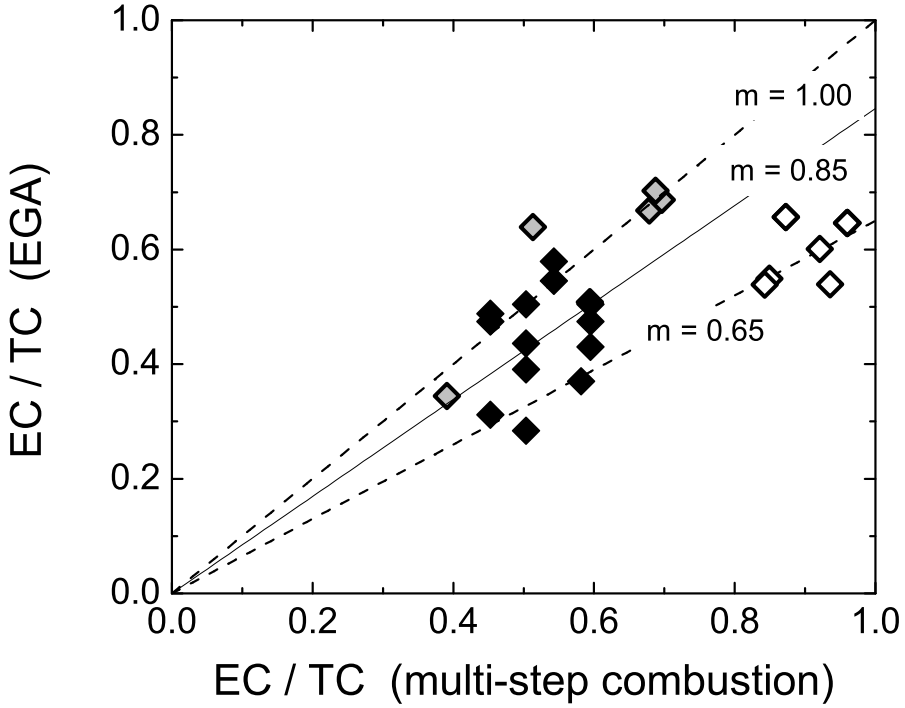

Fig. 2. Correlation of the ratio of elemental carbon to total carbon EC/TC as determined from evolved gas analysis EGA and multi-step combustion as a reference method; symbols represent data for low (open), medium (filled) and high (shaded) fuel sulphur content.

ACPD
5, 2599–2642, 2005

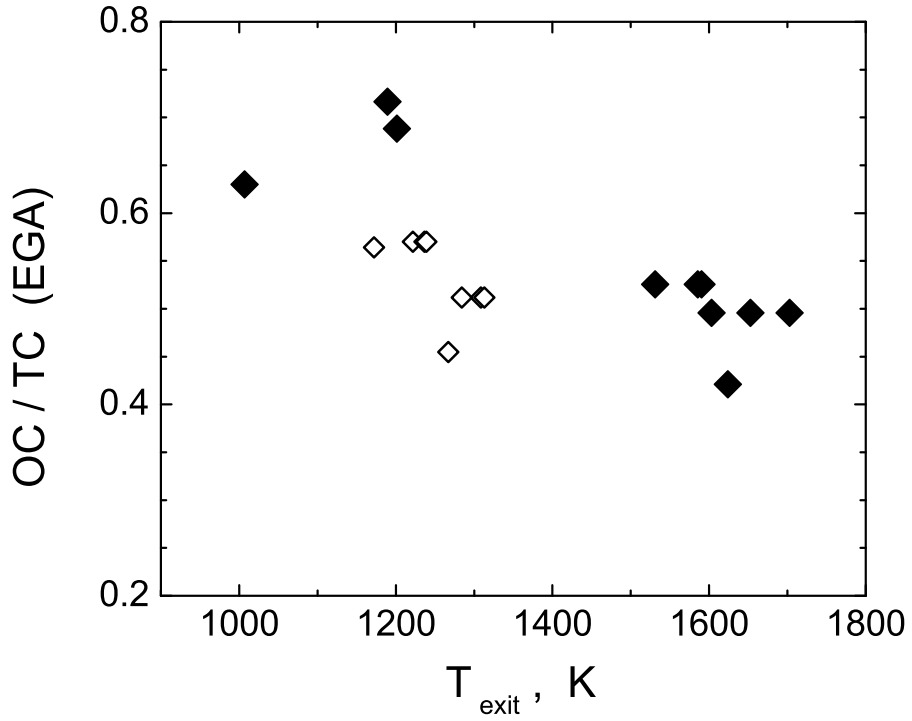

Fig. 3. The organic fraction of total carbon as a function of the combustor exit temperature for the medium FSC case; open (full) symbols indicate data for old (modern) cruise conditions.

ACPD
5, 2599–2642, 2005

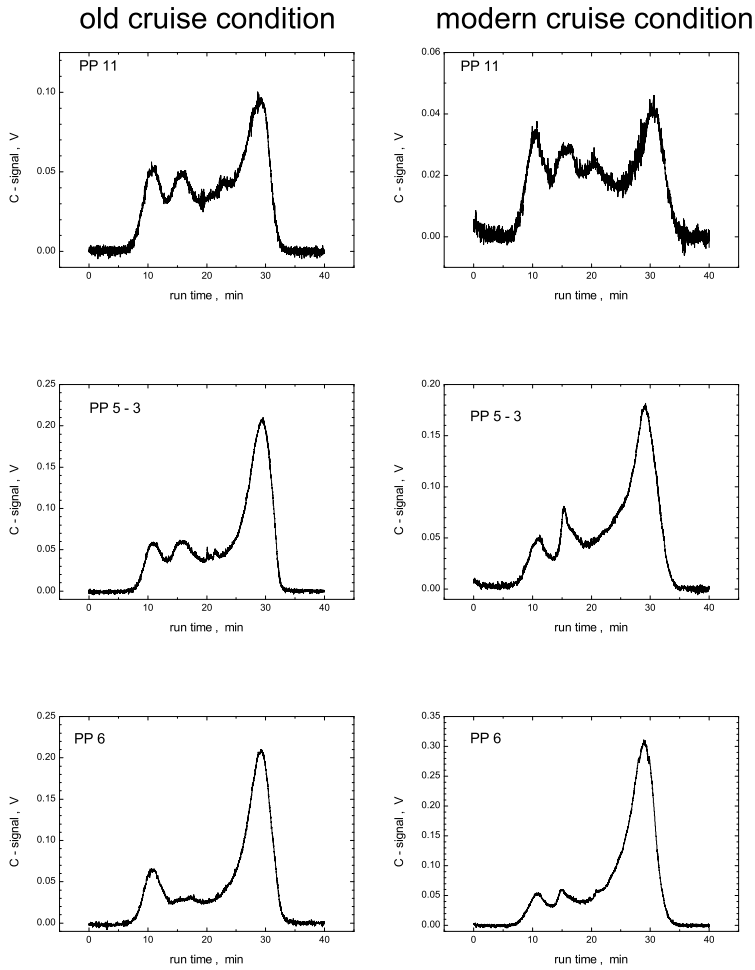

Fig. 4. Thermograms for indicated probe positions for old (left column) and modern (right column) cruise conditions (temperature ˚C=run time×20).

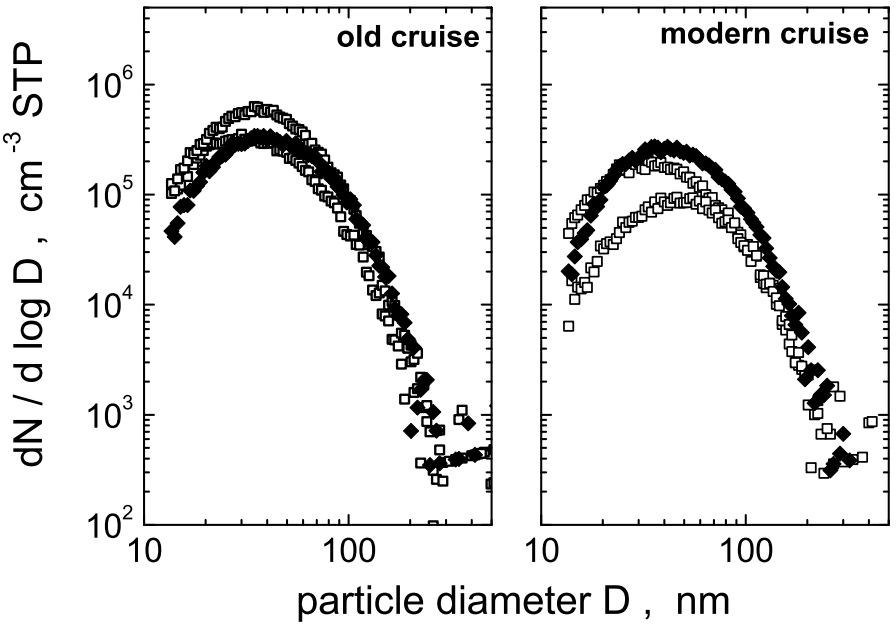

Fig. 5. Particle size distributions measured with an SMPS at edge (open symbols) and centre (filled symbols) positions of the combustor exit area for old and modern cruise conditions.

ACPD
5, 2599–2642, 2005

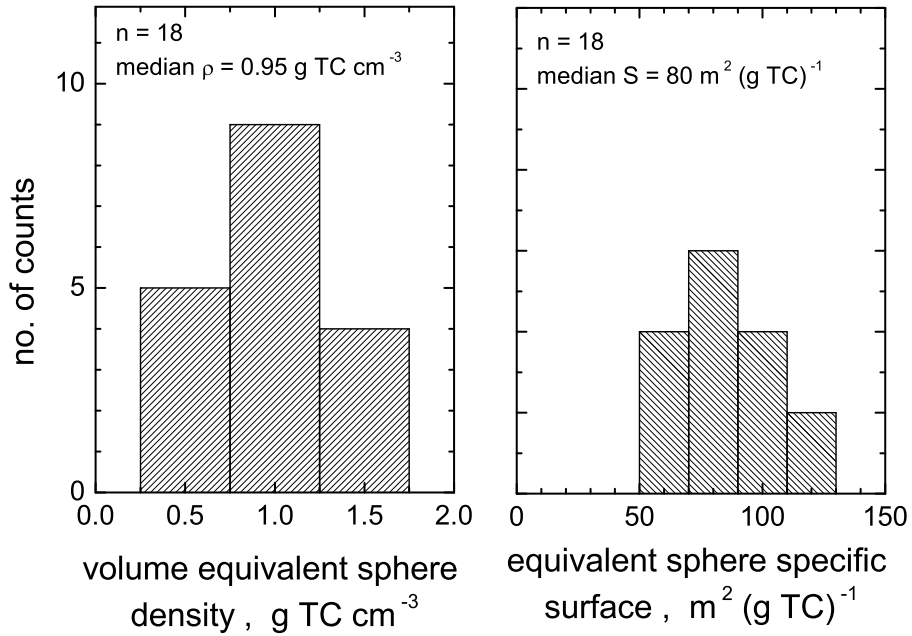

Fig. 6. Density (left panel) and specific surface area (right panel) of the combustion aerosol with respect to total carbon; spherical, particle shape was assumed in both cases.

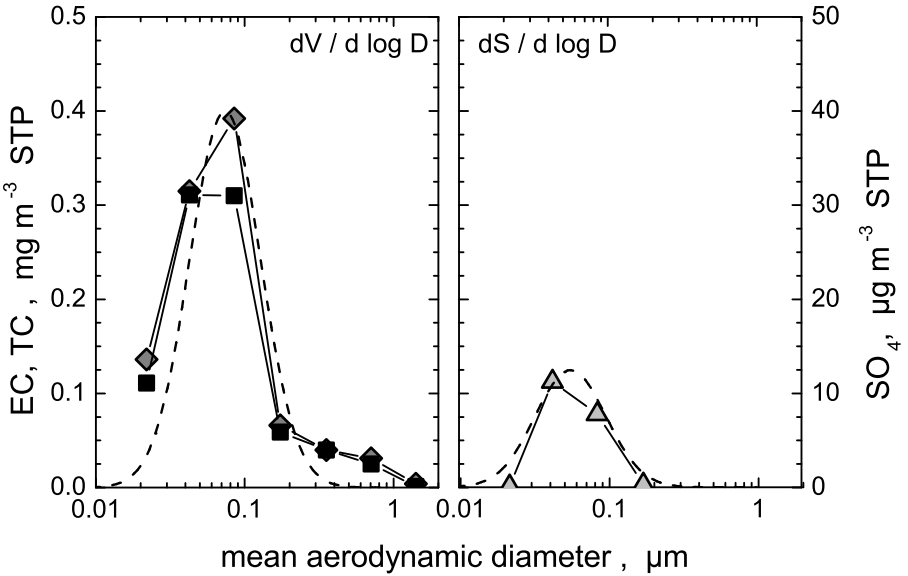

Fig. 7. Size-resolved chemical composition of combustor exhaust particles for high FSC fuel used; left panel shows the mass distribution of total (grey) and elemental (black) carbon together with a volume distribution calculated from measured size DMA spectra; right panel shows the mass distribution of sulphate together with a surface distribution calculated from measured spectra.

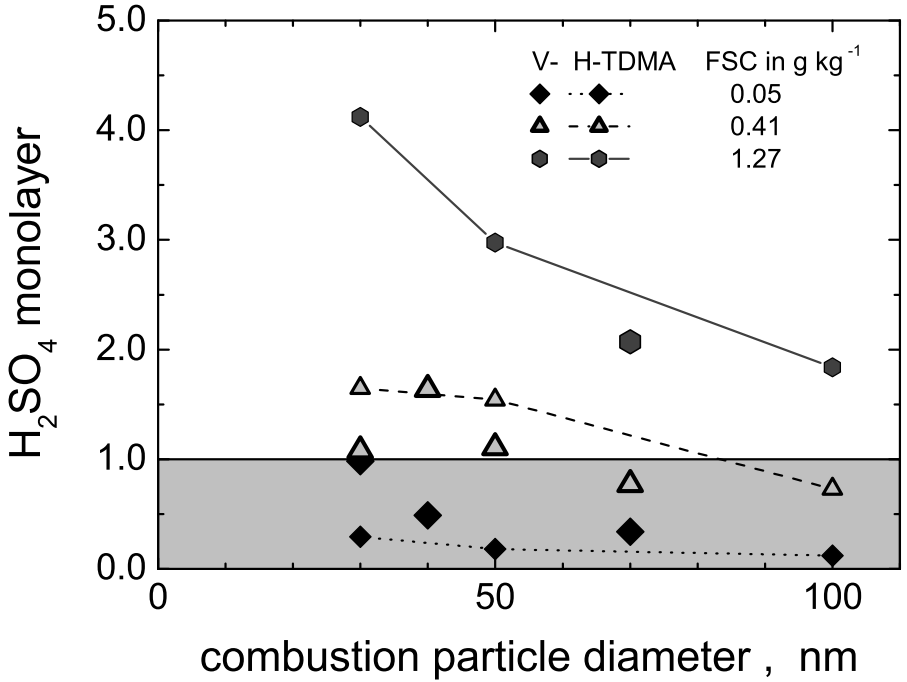

Fig. 8. Coverage of carbonaceous combustion particles in terms of monolayers of H_2SO_4 for different levels of fuel sulphur content FSC; the coating was determined from measurements using Volatility Tandem DMA and Hygroscopicity Tandem DMA methods.

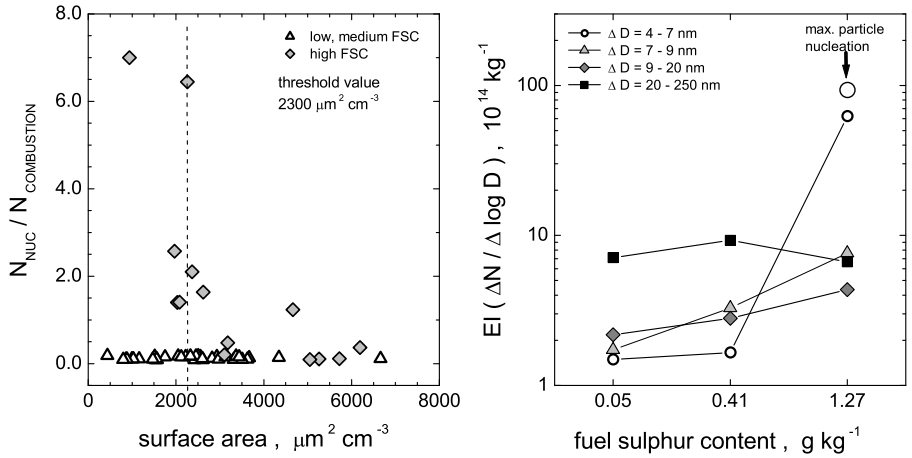

Fig. 9. Left: ratio of nucleated particles N_{NUC} of size D<10 nm to combustion particles $N_{COMBUSTION}$ of size D≥20 nm as a function of the surface area of the pre-existing combustion aerosol; the dashed line denotes the threshold value for particle nucleation of 2300 μm^2 cm^{-3}. Right: number of particles per kg of consumed fuel in denoted diameter bins as a function of the fuel sulphur content.

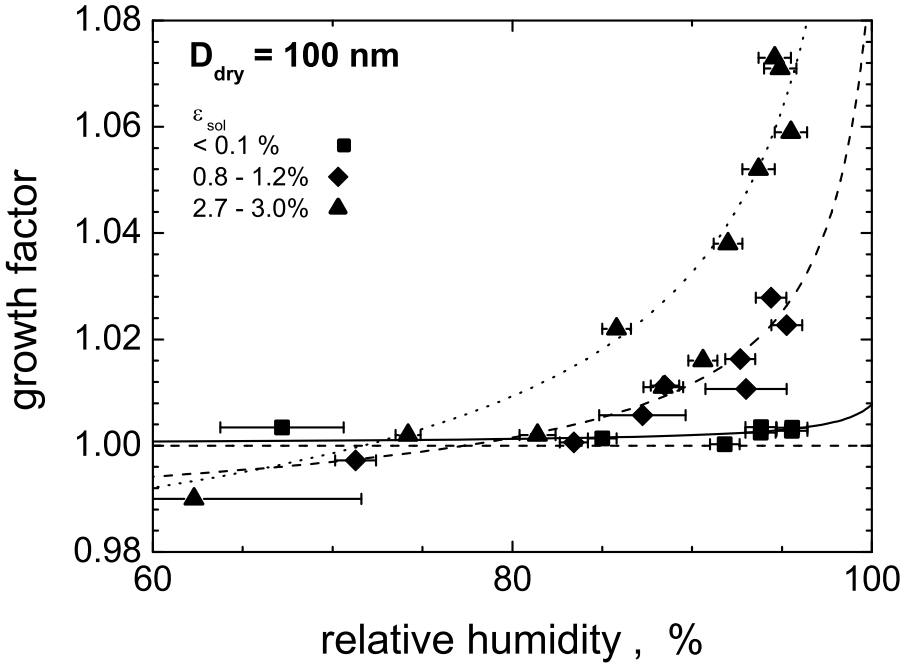

Fig. 10. Humidity growth of particles of initial size D_{dry}=100 nm as a function of relative humidity for low, medium and high fuel sulphur cases; lines represent growth curves determined from Köhler theory for the indicated volume fractions of soluble matter ε_{sol}.

ACPD
5, 2599–2642, 2005

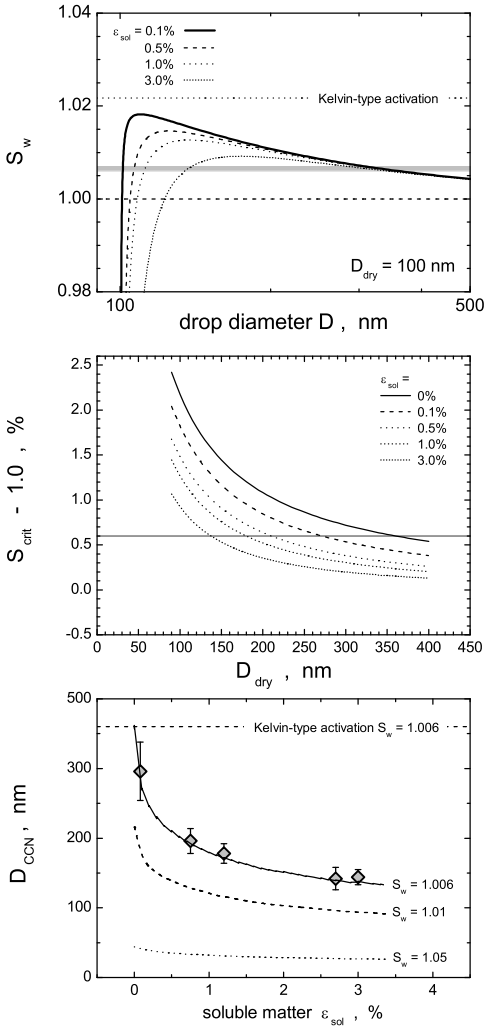

Fig. 11. Top panel: variation of the equilibrium vapour pressure over an aqueous solution drop formed from an insoluble carbonaceous nucleus covered with ε_{sol} volume-% of sulphuric acid in the dry particle state; the grey-shaded area indicates the operation range of the CCN counter. Mid panel: critical saturation ratio for coated particles of dry size D_{dry}, given in % of super-saturation. Bottom panel: activation diameter D_{CCN} for insoluble particles coated with ε_{sol} volume-% of sulphuric acid, symbols represent the measured activation diameters, the lines show results from Köhler theory for the indicated saturation ratios.

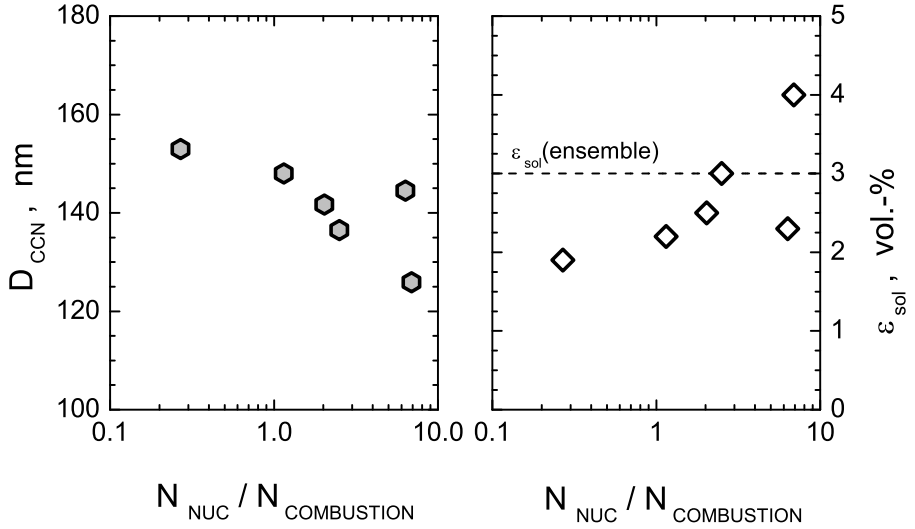

Fig. 12. Left panel: CCN activation diameter D_{CCN} plotted as a function of the ratio of nucleated particles N_{NUC} of size D<10 nm to combustion particles $N_{COMBUSTION}$ of size D≥20 nm for the high fuel sulphur case. Right panel: volume fraction of soluble matter calculated from the measured D_{CCN} values using Köhler theory (Eq. 3); the dashed line represents the ensemble value ε_{sol} determined by the Köhler curve fitting all measurements.

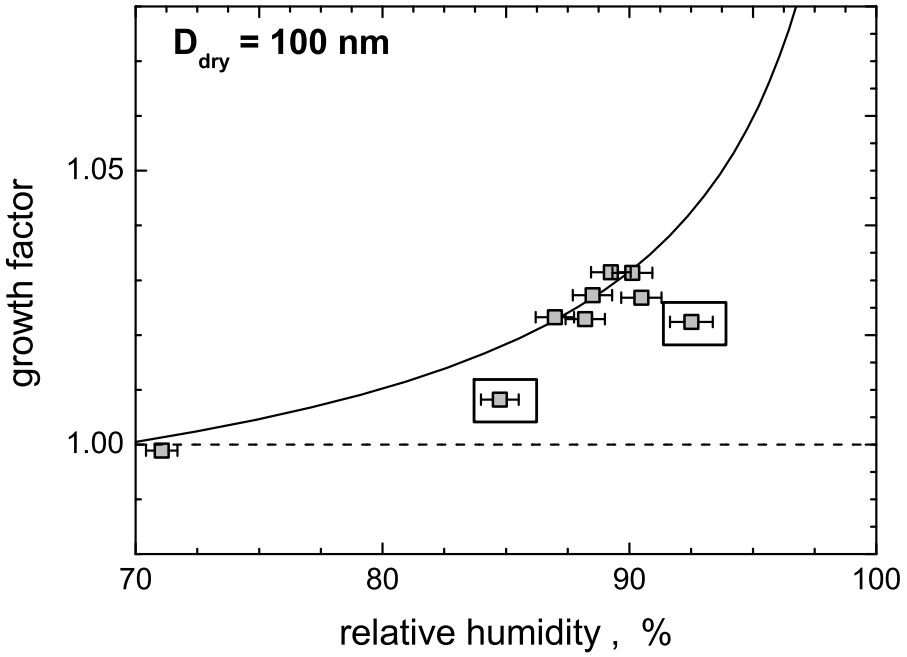

Fig. 13. Humidity growth of particles of initial size D_0=100 nm as a function of relative humidity for the high fuel sulphur case; the indicated data points correspond to sampling points at the edge positions of the combustor exit nozzle plane.

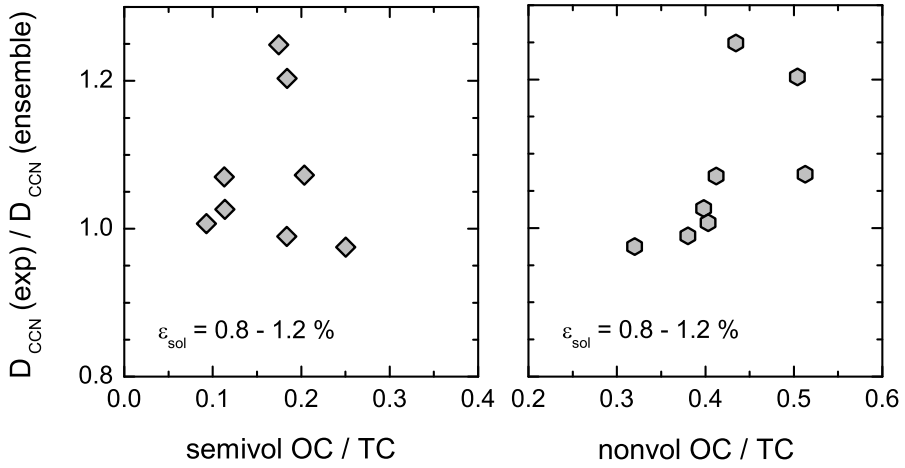

Fig. 14. Ratio of experimental CCN activation diameter to the ensemble CCN diameter determined from humidity growth factors, as a function of the semivolatile OC fraction of TC (left) and the non-volatile OC fraction of TC (right).

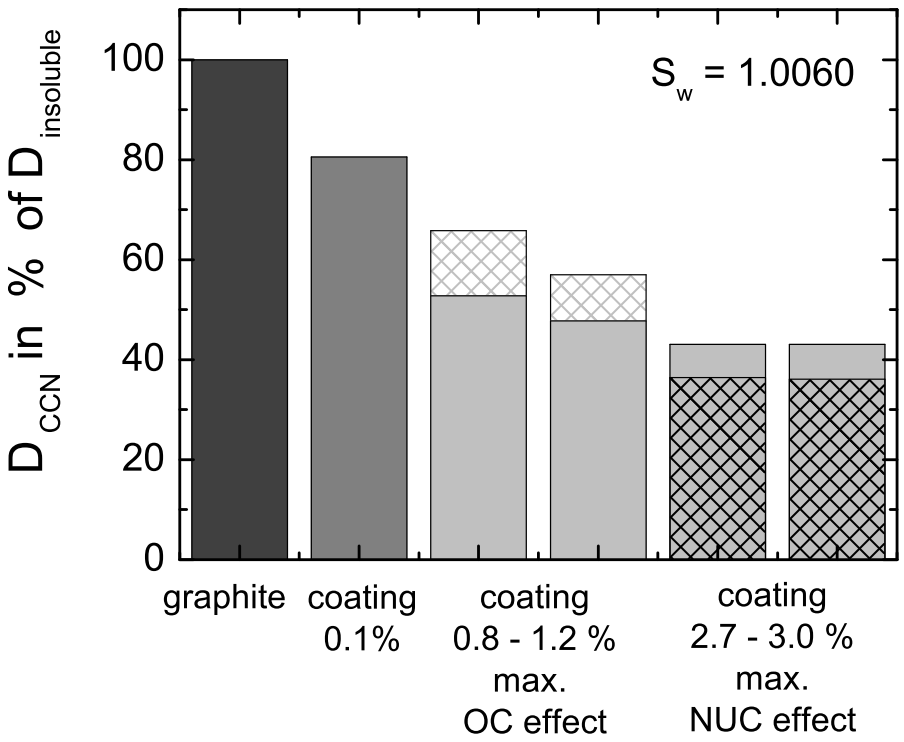

Fig. 15. Relative contribution of particle coating with sulphuric acid to the change in the CCN activation diameter of an initially insoluble graphite particle; the shaded bars represent the increase in D_{CCN} and thus the reduction in CCN activation by a large fraction of non-volatile OC (OC effect) and the further decrease in D_{CCN} and thus the enhancement of CCN activation by particle nucleation-coagulation (NUC effect).